Chapter 4

Results and discussion

4.1 Introduction

A considerable part of this study involved the creation and implementation of the photometry pipeline as was explained in the previous chapter. The success of the implementation of the pipeline on a data set will determine the quality and type of the resulting output. Some comments will be made on the initial expectations of the pipeline and on the success of it on the data set.

As output from the pipeline, differential magnitudes obtained from the PSF photometry lead to the possibility of analyzing each star in the field over the full period of observation. In order to identify each star in multiple images, a master list was created from one single image frame in order to assign a unique ID number to each star which will be used to extract and classify the star in case of an observed variability.

In this chapter, the focus will be on the application of the Lomb-Scargle transform to the data and the results obtained from it. After the application of the Lomb-Scargle transform, some criteria should be established in order to assign a significance to each frequency that was extracted. This significance level should be defined in order to extract a reasonable number of variable sources from the two clusters. The technique to do the above mentioned, that was followed in this study, will also be explained more thoroughly in this chapter.

With known U, B and V magnitudes for a number of stars in NGC 6204 and Hogg 22, obtained by Forbes & Short (1996), B and V magnitudes were calibrated for further comparison and classification. With the calibrated B and V magnitudes, a colour

magnitude diagram was constructed in order to compare results to other studies and to possibly verify cluster membership of some stars.

4.2 Photometry pipeline

Many tasks explained in the previous chapter formed part of the photometry pipeline that was created to be applied to the data set of the two observed clusters. The reasons for creating and using this pipeline on the data became evident from the previous chapter which include the automation of a large number of data processing steps, and the correction of images to one reference frame. The success of the pipeline can be measured by looking at the way the initial problems were addressed and solved. In total thirteen nights of data were collected of which the first three nights were not used due to incomplete header file information, which was only discovered later. The header file is the file created by the software during communication with the CCD camera. Due to the fact that the telescope setup was used for the first observing run, the header file information of the first three nights was not completely set at the time. The header file of each fits image plays an important role in the pipeline processing because of the fact that information can be easily extracted from it.

A second problem that became evident from the data is that the image frames from nights 7, 8 and 9 were scaled to a constant factor of 0.9912, meaning that the distance between any two stars of these nights will show an offset to the master coordinate file used in the pipeline. These problems could however be solved easily but due to time constrains during the data processing a decision was made to use only seven of the ten usable nights of collected data.

By applying the pipeline to the data from nights 5, 6, 10, 11, 12, 13 and 14, rotational and translational transformations were successfully made to all images before the PSF, aperture and differential photometry were performed. The Lomb-Scargle transform could then be performed on the resulting time series data of each star in order to search for possible periodic behaviour in the data.

4.3 Periodicity extraction

4.3.1 Lomb Scargle periodogram

When applying the Lomb-Scargle transform to time series data, the result is the power associated with each frequency extracted from the time series. The significance of the extracted frequency can be indicated by its corresponding power, where the power is given by

$$P_N(\omega) \equiv \frac{1}{2\sigma^2}\left(\frac{\left[\sum_j (h_j - \bar{h})\cos\omega(t_j-\tau)\right]^2}{\sum_j \cos^2\omega(t_j-\tau)} + \frac{\left[\sum_j (h_j - \bar{h})\sin\omega(t_j-\tau)\right]^2}{\sum_j \sin^2\omega(t_j-\tau)}\right), \quad (4.1)$$

where ω is the frequency, t_j are the times at which the data is evaluated, $\bar{h}$ and σ^2 are the mean and variance respectively and the constant τ, which makes $P_N(\omega)$ independent of shifting all the t_i's by any constant, is defined by $\tan(2\omega\tau) = \frac{\sum_j \sin 2\omega t_j}{\sum_j \cos 2\omega t_j}$ (Press et al., 1992).

However, it is not permissible to simply come to the conclusion that there is a periodic signal in a time series if there is a strong peak in the periodogram. A time series consisting of pure noise may also result in the periodogram showing a "strong" peak at a particular frequency. It is therefore necessary to somehow discriminate between a strong peak due to noise and a strong peak due to a real periodic signal in the time series, which now raises the question of what can be expected from a time series consisting of pure noise.

An important point to understand here is that in all cases an observed time series is only one possible realisation of the time series of the specific physical phenomenon. The reason for this is that a repeat of the measurements to construct the time series will in general not result in the same values at the given observation times. This is due to either measurement errors or intrinsic random fluctuations at the source. As a consequence of this behaviour, the power at a specific frequency in the periodogram will not be the same for all possible realisations of the time series. Even if there is a real periodic signal with frequency ω in the time series will the power at that particular frequency not be the same for different realisations of the time series. Since the different realisations of the time series is statistical in nature, will there be a distribution of powers for the "peak" associated with the frequency ω.

With this in mind, some level should now be defined in order to accept those sources as periodic that appear above a specific cut off level. However, it is important to keep in

mind that periodicity of a source cannot be rejected below this level. The cut off level can only be used to assign a significance to a specific source.

4.3.2 Significance level

The identification of an underlying periodic signal in the time series is usually done by identifying the frequency with the most power, ie. the strongest peak in the periodogram. Thus, to be able to distinguish whether this strongest peak is due to noise or a real signal, is it necessary to know what the distribution is of the power of the strongest peak in the periodogram of a time series of pure noise. In the language of statistical inference, this distribution is known as the distribution of the test statistic under the null hypothesis where in this case the null hypothesis is that the time series is just that of pure noise. The alternative hypothesis is that there is a periodic signal in the time series. The test statistic in this case is the power of the strongest peak in the periodogram. It is on the basis of the value of the test statistic, the power of the strongest peak in the periodogram, that a decision will be made whether the time series is just pure noise or whether it contains a periodic signal, which can then also be used to assign periodic significance to a specific source.

The distribution under the null hypothesis can be constructed using a Monte Carlo simulation of the time series, with the same times as the observed data but containing only random Gaussian noise. In practise this means that a very large number of realisations of the time series with pure noise is generated and in each case the power of the strongest peak in the corresponding periodogram is recorded. With these numbers it is possible to calculate what the probability is that the strongest peak in the periodogram have a power greater than a given value, ie. to construct the cumulative distribution function.

The procedure that was followed in this study to determine the significance level involved applying the Lomb-Scargle transform to 10^4 realisations of the random noise time series, where the power of the strongest peak in each periodogram were found. One such realisation of the time series resulted in the periodogram shown in Figure 4.1, which comprises of frequencies extracted with different powers. The cumulative distribution of Z_{max} is shown by the black solid line in Figure 4.2. It is seen that for small values of Z, the probability that $Z_{max} > z$ is equal to one. However, $P(Z_{max} > z)$ decreases very rapidly as z increases. For example, it is seen that $P(Z_{max} \geq 8)$ is about 0.15. In terms of testing the null hypothesis it means that if the power of the strongest peak in the periodogram has a value of 8, that the probability of this value being due to pure noise is 15%. Obviously, one would like to make this probability as small as possible in order to reject the null hypothesis with confidence. Using the data to construct the

cumulative distribution function it was found that $P(Z_{max} \geq 13.4 = 10^{-4})$ for the case of pure noise. Should one therefore find that the power of the strongest peak in the periodogram is greater than 13.4 it would mean that the probability of such an event, being due to pure noise, is less than 10^{-4}. The null hypothesis is therefore rejected at a confidence level of 99.99%. For further reading on this topic see Frescura et al. (2007, 2008)

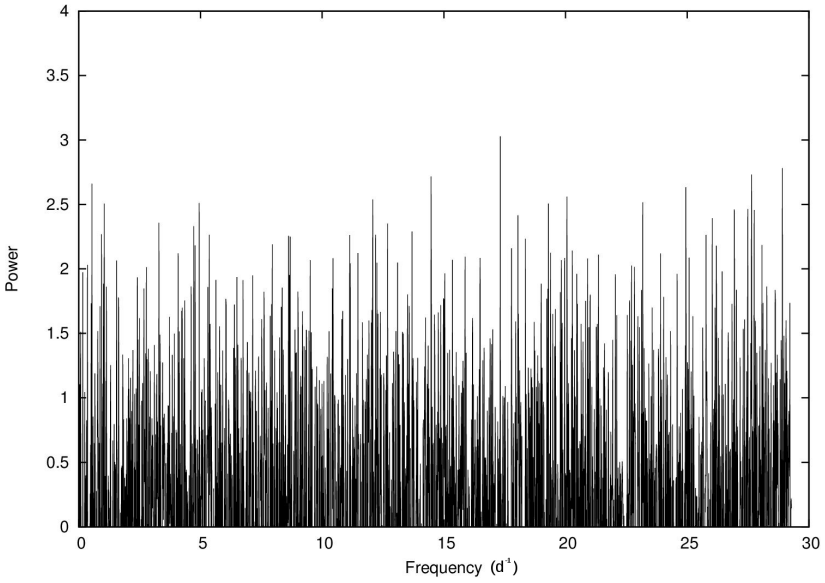

FIGURE 4.1: Periodogram of a random noise time series with the same times as the observational times.

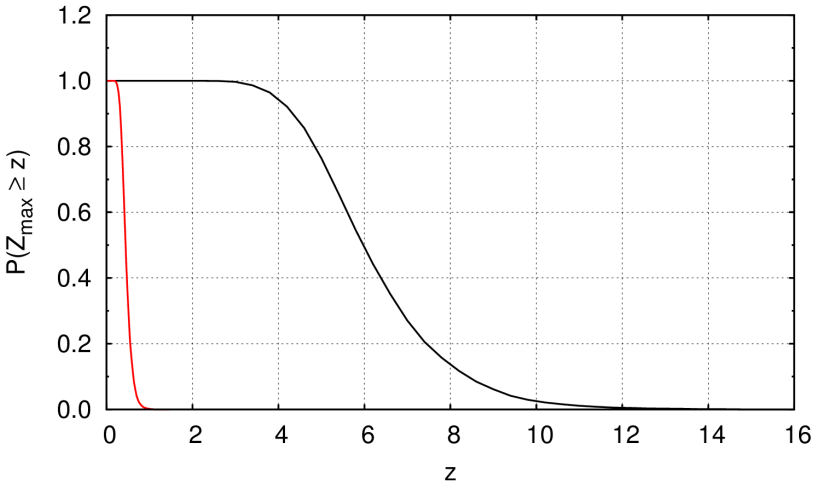

FIGURE 4.2: Spectral power distribution with normalized distribution (red) of random noise time series representing the null hypothesis of the Lomb-Scargle periodogram

According to this distribution, if a spectral power value of 13.4 is extracted from the periodogram of a source, it has a probability of around 0.01% to originate from pure noise. The spectral power was normalized to a value of 1, which corresponds with a confidence level of 99.99% that the signal is not from the noise. The normalization was done in

order to simplify the spectral power scale together with further computations done on the data set. The normalized distribution is indicated by the red line in Figure 4.2, and was used as reference to filter through all sources, according to the highest power, which corresponds to the most prominent frequency in the periodogram of a source.

A numerical experiment was done to test the sensitivity of the Lomb-Scargle transform to a periodic signal in a fixed noise level. By adding random noise from a Gaussian distribution to a sine function, sampled at the observation times, and repeatedly decreasing the amplitude of the function, it is possible to get an indication of the smallest signal to noise ratio (SNR) from which a periodic signal could be extracted when applying the Lomb-Scargle transform. Figure 4.3 shows the normalized spectral power extracted as a function of the SNR. In this case the SNR was defined as the ratio between the amplitude of the input sine function and the standard deviation of the Gaussian noise. By applying the Lomb-Scargle transform to the sine function, the retrieval accuracy

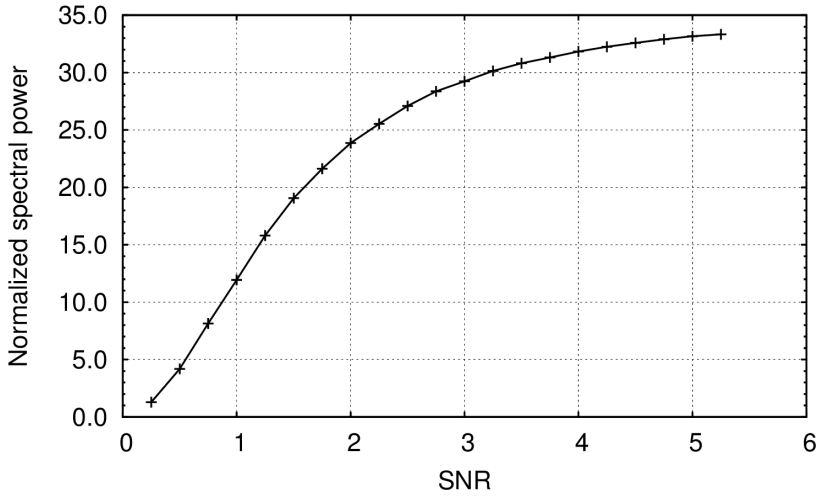

FIGURE 4.3: The normalized spectral power of a frequency obtained from a sine wave within a variable noise level. The SNR is defined to be the ratio between the amplitude of the input sine function and the standard deviation of the Gaussian noise.

can be indicated by the relative deviation from the input sine frequency as function of the SNR as defined above. This is shown in Figure 4.4, where it is clear that very low SNR signals can still be extracted from noise using the Lomb-Scargle transform. From Figure 4.4 it can be seen that the deviation of the retrieval frequency from the input frequency is not zero, even at high SNR values, which can be explained by the fact that the frequencies in the periodogram can only have discrete values.

By now using a 99.99% confidence level on the data set as defined above, a total of 1562 sources were found to be variable under the chosen criteria. The importance of the null distribution becomes clear when a level needs to be chosen in order to label sources

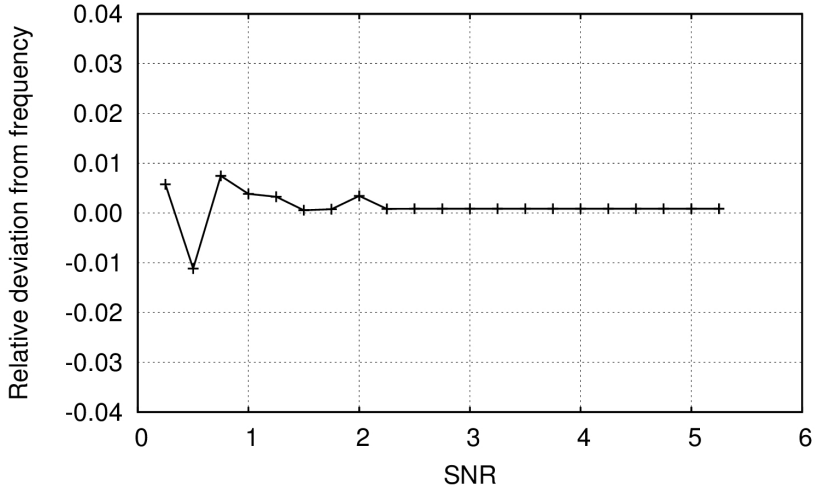

FIGURE 4.4: The retrieval accuracy presented as the relative deviation from the input signal as a function of SNR (as defined above), when applying a Lomb-Scalgle transform on a sine wave in a variable noise level.

below it as insignificantly variable. However, the question of where the cut should be made is a highly subjective one due to the the following arguments:

- With the above explained method an ideal case is assumed where the source exhibits sinusoidal periodicity. However, the true nature of periodic or variable sources may include different periodic modes which will cause deviation from the ideal case of sinusoidal periodicity.
- The five stars that were used during the differential photometry process, which need to be constant, will in reality never be constant, but varying to some extent.
- The probability of finding a truly constant star in nature is highly unlikely, likewise is the probability of finding a star with no periodic variability. This can be explained by the analogy of a star which is variable at a level of 2.5 milli-magnitudes which is observed with a detection threshold of 5 milli magnitudes, in which case the star will appear to be constant except when lowering the detection threshold below the amplitude of variation. The same applies for the periodic case in which a decrease in confidence level will only present sources with lower spectral power values in their periodograms and less significant periodicity which can eventually be totally included in the noise level of the periodogram. This will happen if either the star is not well sampled or the periodicity is very weak.

Thus, in reality the choice of spectral power cut off= 13.4 may not be the optimal choice. It is necessary to determine such a value by careful inspection of the specific data set under study.

A distribution of the variable sources above the normalized spectral powers of 1, 5, 10 and 11 is shown in Figure 4.5, where the number of stars that satisfy each spectral power criteria is indicated on each graph. These distributions can assist in choosing a better spectral power cut off for this particular study. The graph in the top left hand corner in Figure 4.5, shows the distribution of stars with normalized spetral power greater than one. These 1562 stars amounts to almost 50% of the total number of stars detected from the two open clusters under study. Stars with a normalized spectral power of more than five, contribute to around 10% of the total stars while 2% have normalized spectral powers above 10, and 1% above the value of 11.

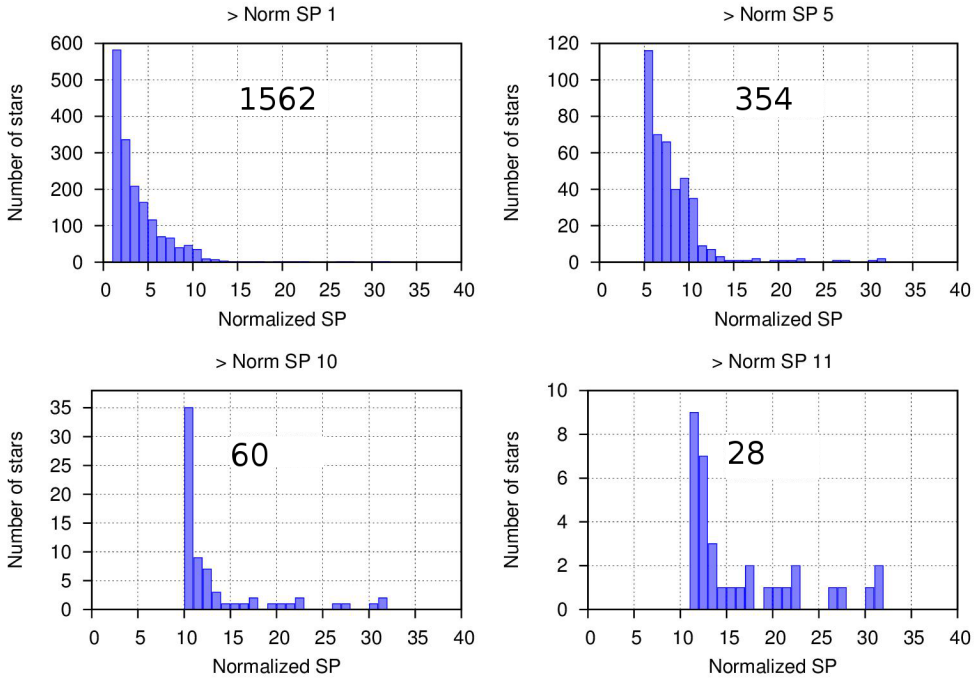

FIGURE 4.5: The distribution of variable sources found above the indicated normalized spectral power value.

According to Paczynski & Pojmanski (2000), a few percent of all stars are detectably variable, where around 90% of all variable stars brighter than 12th magnitude have not been discovered yet. In another study done by Nichols et al. (2010), where the variable guide stars from the Chandra X-ray space telescope were studied, it was found that almost 9% of all guide stars with spectral types O and B were in fact variable, which is shown in Table 4.1. With only this in mind, and the fact that the two open clusters contain a large number of O and B type stars, it can be statistically expected that the number of significantly variable stars found in these two clusters should be around 10% of the total number of stars.

Another important factor which should be taken into account when choosing a spectral

Spec type	No. of stars	No. of variables	No. of previously unknown variables	No. of pulsators	No. of Eclipsing binaries	No. of indeterminate
O	80	7	5	1	0	4
B	1444	121	49	25	27	55
A	3881	177	111	78	33	55
F	6360	173	98	78	38	52
G	7257	45	24	7	12	19
K	13616	26	16	4	5	12
M	1332	9	1	8	0	1

TABLE 4.1: Distribution of the VGUIDE variable stars used as guide stars by the Chandra X-ray telescope. Data obtained from Nichols et al. (2010)

power cut off, is the choice of the constant/reference stars used in the differential photometry process. The highest observed normalised spectral power of any of the reference stars is at a level of 4.9. When taking these two facts into consideration, a decision was made to use a significance level located just above the five stars used as constant/reference stars during the differential photometry process. This implies that all sources with normalized spectral power lower than those of the differential photometry reference stars will be regarded as insignificantly variable. This means that the level should be set at a minimum normalised spectral power value of 5 where this value also corresponds with the crude variability percentage of 10% in the cluster. The normalized spectral value of 5 implies an insensibly high confidence level according to the distribution in Figure 4.2, which indicates that the spectral power values should just be used as a reference to determine a sensible periodicity cut off level. This level will, however, be different for each individual study. It should, however, be noted that the periodogram of a constant star does not resemble that of the Gaussian noise periodogram as would be expected. This gives reason to believe that the data behaves differently from what would be expected from pure Gaussian noise.

By using such a high confidence level, the possibility of excluding less significantly periodic sources with lower amplitude light curves also exists. This happened with two bright, high SNR sources, showing low amplitude variations, but which could be detected by inspection of their light curves (Figure 4.6). These two variable stars also turned out to be two new β Cephei candidate stars, which will be presented later in this chapter. In conclusion to this argument it can be said that simulations of an ideal case can only be used as a guideline in identifying possible periodic stars where adaptations should be made afterwards on the periodic significance criteria.

4.3.3 Inspection of extracted frequencies

After identifying all variable sources from the data set, inspection of the extracted periods showed a spurious period of 0.49631 days, that appeared a few times throughout

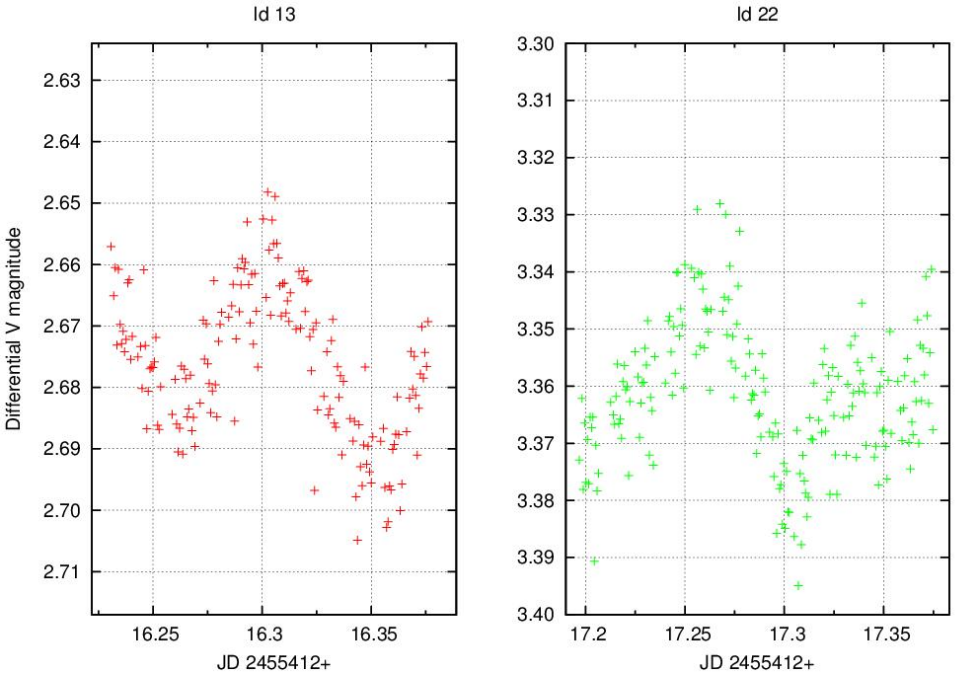

FIGURE 4.6: Differential magnitudes shown for the two β Cephei candidate stars.

the list of variable sources. Because of the highly unlikely possibility of obtaining the exact same frequency from more than two different and independent sources, the light curves of these sources were compared to search for a common property.

Sources with the highest normalized spectral power values were extracted, where the inspection of the light curves of these sources revealed a big increase in the magnitude of the source towards the end of each night. Secondly, the position of each of these sources were checked to see where they are located in the field. One clear commonality between their positions in all cases were found to be the close proximity to very bright stars.
The phenomenon of increasing magnitude can be explained by the fact that the atmospheric seeing conditions usually deteriorated throughout the night, with the worst conditions observed a few hours before sunrise. The deteriorating seeing caused an increase in the FWHM of the brighter star, where the close by faint star was affected by the expanding wing area of the bright star, leading to inaccurate photometry. Thus, all the stars with a period of 0.49631 days were removed from the list of candidate periodic stars.

4.4 Classification of variable sources

In order to classify a variable source from the data, direct inspection of the light curve together with knowledge of the spectral type can be of great importance. The inspection

of the light curves together with the accompanying periodogram is important in order to obtain the correct frequency for each mode observed in the light curve.

4.4.1 Frequency identification

By applying the Lomb-Scargle transform on a data set, it is important to note that it will be very successful on sinusoidal periodic data. However, some stars like eclipsing binaries, deviate strongly from sinusoidal variation because of the existence of more than one minimum and maximum during an orbital period. If the consecutive minima or maxima are at a similar amplitude, then the Lomb-Scargle transform will most likely extract double the orbital frequency or halve the orbital period. For this reason it is very important to visually inspect the light curve for different frequencies which can be present and not to blindly accept the raw results of the Lomb-Scargle periodogram.

Another important aspect of frequency extraction to take into account is the occurrence of spectral leakage, also known as aliasing. Alias frequencies occur in periodograms because of unevenly spaced data, gaps in the sampling of data even if it is regularly sampled and the limited dimension of the data window in which observations were done (Horne & Baliunas, 1986). In astronomical data, the occurrence of frequencies as daily or monthly aliases are quite common, where daily aliases were also detected in this study. In a study done by Horne & Baliunas (1986) on the analysis of unevenly sampled time series, a useful method is explained to verify if a significant frequency peak is an alias of another significant frequency. This method involves subtracting a sine curve with a frequency of the most significant peak in the periodogram and then recomputing the periodogram. According to Horne & Baliunas (1986), this procedure minimises the problem of aliasing to a great degree.

This technique, used to distinguish alias frequencies from true frequencies, was applied to the present data with mixed success. Figure 4.7 shows a snapshot view of the application of this technique to the data of the known β Cephei star in Hogg 22. The top left hand frame (red) shows the original periodogram with no frequencies subtracted. By inspection of the periodogram, daily aliases of 1.4, 2.4, 3.4, 4.4, 5.4, 6.4 and 7.4 d^{-1}, which are indicated on the graph, can clearly be seen. If this technique is successful, it is expected to see the dissapearance of the alias frequencies if the true frequency is subtracted. To show the effect of this technique, the three strongest frequencies of 3.4, 4.4 and 5.4 d^{-1} were consecutively subtracted. The periodogram was recomputed after each subtraction to see whether the alias frequencies were removed. The graph to the right of the original (green), shows the periodogram after the subtraction of a frequency

of 5.41 d^{-1}, where the daily aliases are still clearly visible. These aliases were still present after the subtraction of the 3.45 d^{-1} frequency in the third frame (blue). The last frame shows the periodogram after subtraction of the 4.45 d^{-1} frequency, which is also believed to be the true frequency. A collapse of the alias structure can be seen where strong daily aliases are absent. However, when this technique was applied to stars which exhibit eclipsing binary light curve profiles, it was less successful. Possible reasons for this can be explained by referring to the shape of the light curve and the frequency of occurring eclipses.

- Some of the eclipsing binary light curves deviate substantially from sinusoidal variation.
- When the eclipse did not occur during a particular observing night, subtracting a specific frequency from the whole data set will result in the creation of that same frequency in the night where no eclipse was observed.

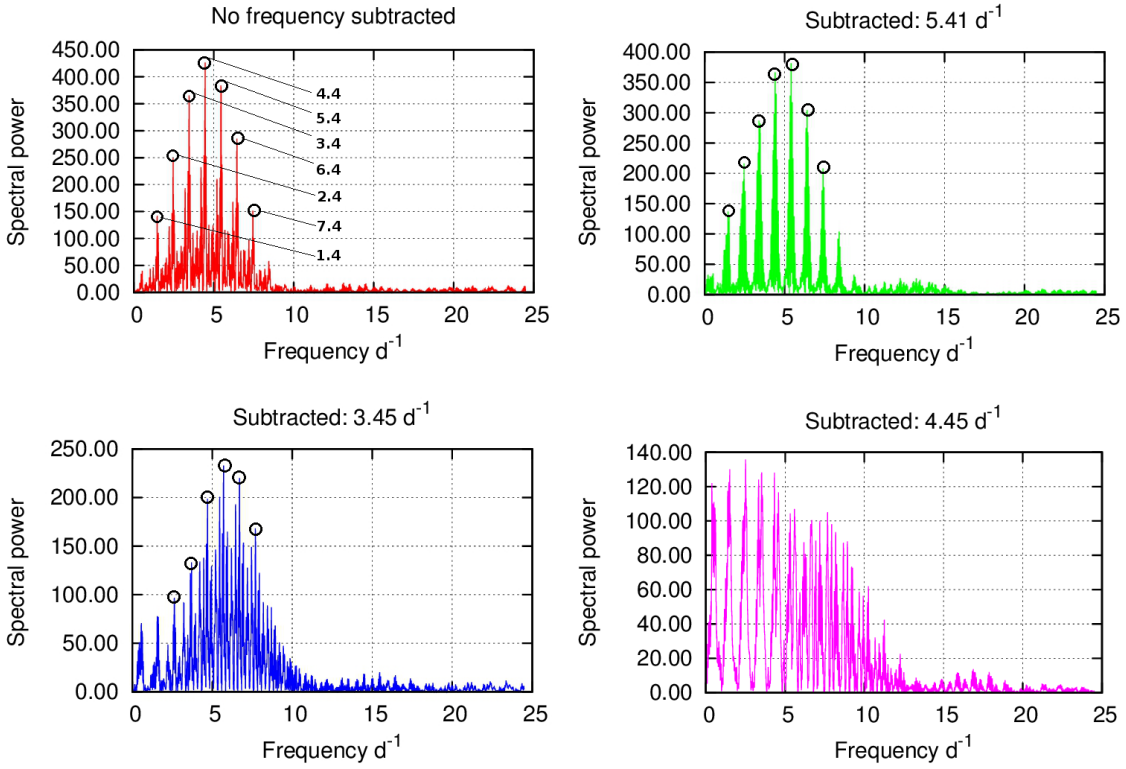

FIGURE 4.7: A set of periodograms from the data of id11 (β Cephei star), showing the periodogram after the subtraction of a sine wave with frequency as indicated. This method was used to identify the true frequency, shown by 4.45 d^{-1}, resulting in a periodogram without the alias frequency pattern observed in the initial periodogram.

4.4.2 Identification of high amplitude variable sources

The light curves and periodograms of a few of the highest amplitude variable sources, found from the data of NGC 6204 and Hogg 22, are shown in Figures 4.8, 4.9, 4.10 and 4.11. Valuable insight into the identification of light curves from specific periodic sources was obtained from Prof Andrzej Pigulski. This allowed for the possible classification of some sources according to variability period and the profile of the light curves. Comparisons were also made to light curves presented on the American Association of Variable Star Observers (AAVSO) website and the NASA Kepler website (American Association of Variable Star Observers, 2012, Nasa Ames Research Center, 2011).

From Figure 4.8, the first light curve titled id11 shows the light curve obtained from a single night of the known β Cephei star in Hogg 22. The periodogram of each source is shown on the right hand side of the light curve, which is computed from data obtained over the total observing period. A period of 0.2243 days was recorded for this β Cephei star which is very close to the period of 0.2241 found in the ASAS 3 survey by which it was discovered (Pigulski & Pojmański, 2008). On the particular night of the displayed light curve the photometric accuracy on this β Cephei star was calculated to be 4.8 milli magnitudes as derived from the standard deviation of the residuals after fitting the data.

The second light curve and periodogram, titled id16, belongs to a possible eclipsing binary system, which is a good example of a source that deviates strongly from a sinusoidal light curve by displaying different amplitude eclipses. Although the most prominent frequency is indicated, from the periodogram, to be 1.684 cycles per day, the Lomb-Scargle transform extracted double the frequency because of the different eclipsing amplitudes. The frequency of $(1.684/2)\mathrm{d}^{-1}$ yields an orbital period of 1.187 days.

Figure 4.9 shows light curves and accompanying periodograms of id726 and id83, where id726 is identified as a possible EA (Algol-type) eclipsing system with period of 0.7304 days. The EA-type system is known to consist of spherical to somewhat ellipsoidal components, where the eclipse boundaries are clearly defined in the observed light curve. A nearly constant region can be seen between consecutive eclipses. Periods ranging from 0.2 - 10000 days are possible with light variation of several magnitudes (The International Variable Star Index, 2012). Only one eclipse was observed for id83 during the 13 days of observation.

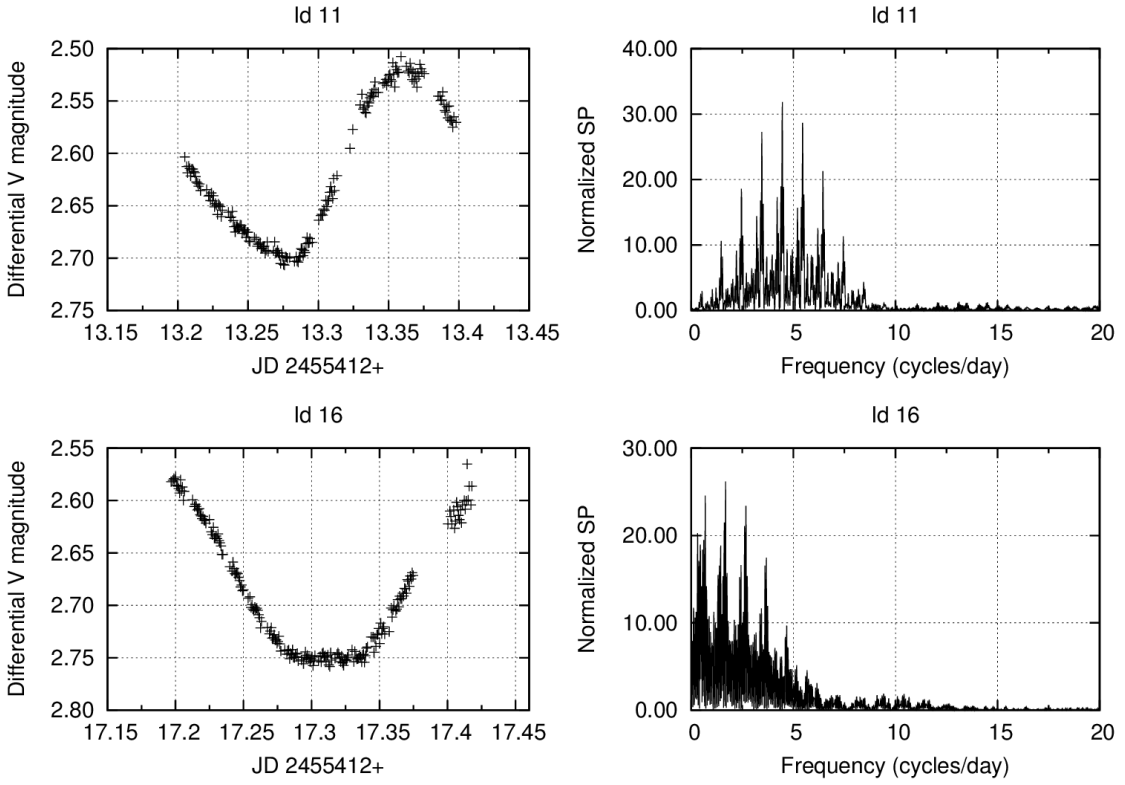

FIGURE 4.8: Light curves and corresponding periodograms of the β Cephei star id11 with period of 0.22426 days and eclipsing binary id16 with an orbital period of 1.187 days.

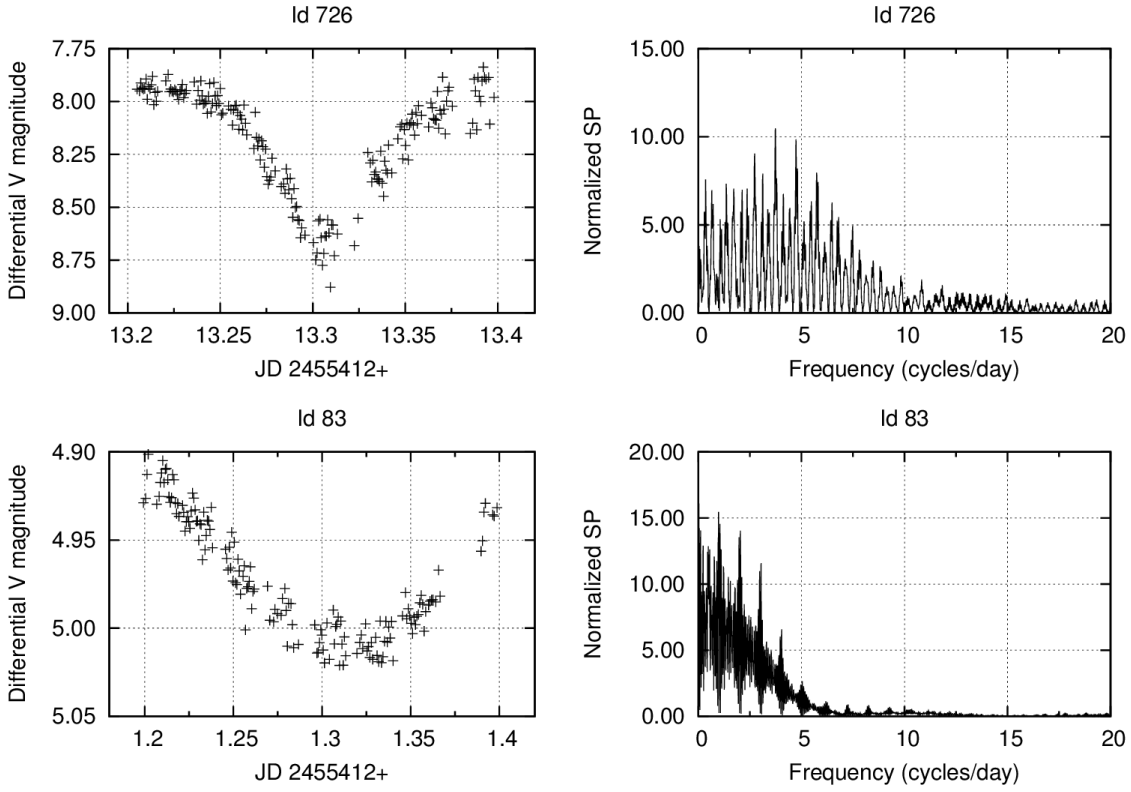

FIGURE 4.9: Light curve and periodogram of id726. A one day alias of double the frequency was observed in the periodogram leading to a period of 0.7304 days. The light curve of id83 showing only one eclipse during the 13 days of observation, therefore with no period associated with a recurrence

The third set of light curves, shown in Figure 4.10, again show the light curve of a possible eclipsing binary, id1081 with a period of 0.4017 days together with another possible EA-type binary system, id1516 with an observed period of 0.8409 days.

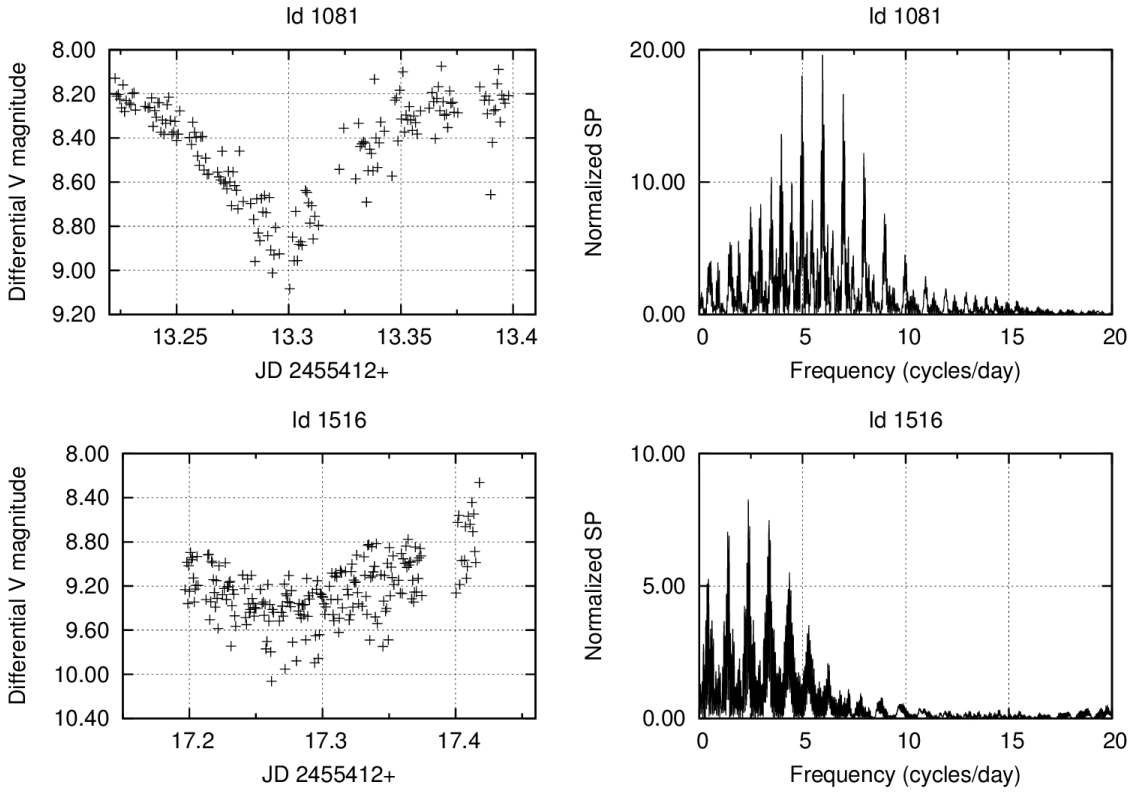

FIGURE 4.10: A one day alias of double the eclipsing frequency was observed in the periodogram of id1081 showing a period of 0.40172 days. For the possible EA-type eclipsing variable, id1516, double of the eclipsing frequency was observed which gives a frequency of 1.189 d^{-1} or a period of 0.8409 days.

The last set of light curves presented in Figure 4.11 includes a possible Bp/Ap-type star, id35. In a recent study done by Bailey et al. (2012), similar variable behaviour was observed from a star, which is believed to be a rapidly rotating Bp star. According to Bailey et al. (2012), the star possesses a very strong quadrupolar magnetic field which varies as the star rotates and creates a non-uniform distribution of elements on the stellar surface.

The star id1415, may possibly be associated with the class of EW, W Ursae Majoris-type, eclipsing variables. These binary systems usually exhibit periods shorter than one day. It is also very difficult to note an exact start or end time of the eclipse from the light curve, where the primary and secondary minima are very similar in depth (The International Variable Star Index, 2012).

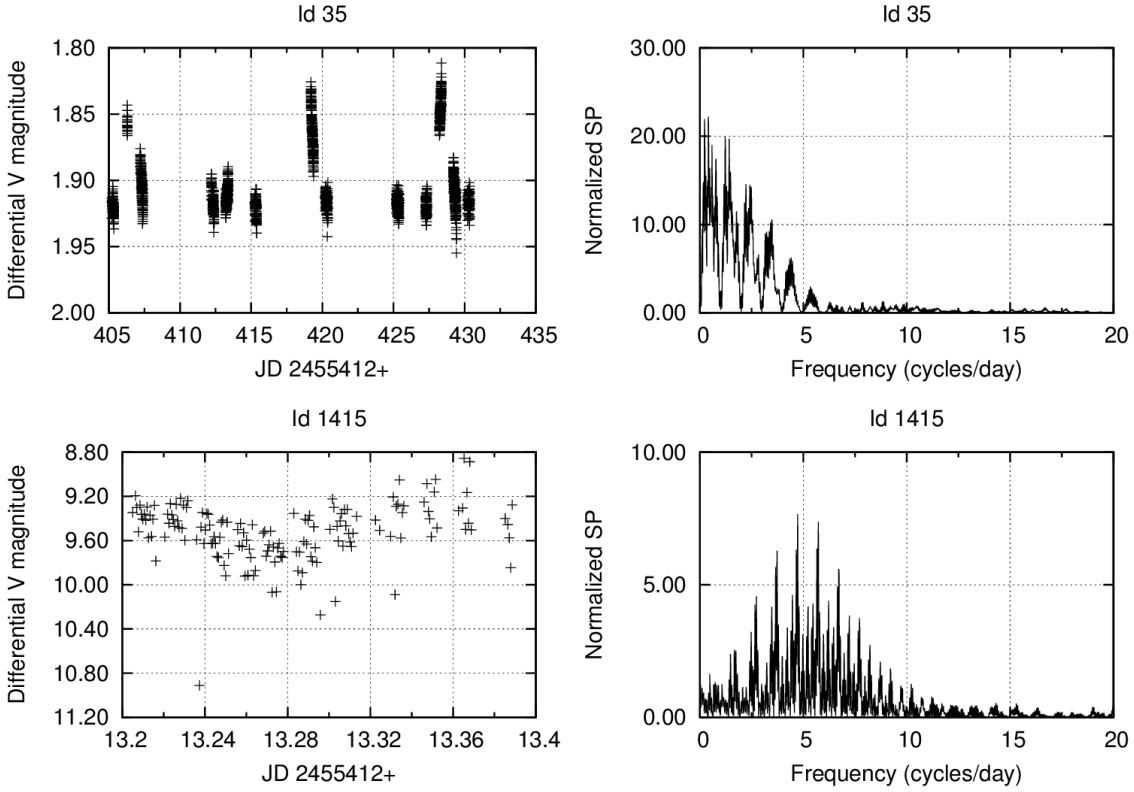

FIGURE 4.11: The possible Bp-type id35 showed a increase in magnitude on three different nights with a possible period of 2.4547 days. The period observed for id1415 was a daily alias of double the true frequency, resulting in a period of 0.34944 days

A few other interesting variable sources which are not shown graphically, includes id17, which is a possible SPB star (slowly pulsating B star) with a possible period of 0.641 days. In order to identify it as an SPB star, the spectral type needs to be determined, where SPB pulsators are observed to be main sequence B2-B9 stars. Multiple periods may be observed in these stars ranging between 0.4 - 5 days (The International Variable Star Index, 2012).

4.5 Calibration of instrumental magnitudes

In order to do the variability search conducted in this study, no need existed to calibrate the obtained instrumental magnitudes to a standard system. However, in order to classify the variable sources, it is important to know the colour and spectral type of a source.

The instrumental magnitudes were calibrated to a standard system in order to construct a colour magnitude diagram on which all stars from both clusters could be indicated. This also presented the opportunity to possibly verify cluster membership of individual stars based on their positions on the diagram. In a study done by Forbes & Short (1996), U, B and V photometry were obtained for NGC 6204 and Hogg 22 which were used to calibrate only B and V band magnitudes. The transformation equations used to calibrate the B and V instrumental magnitudes are given by

$$\begin{aligned} V - v &= A * (b - v) + B \\ B - V &= C * (b - v) + D \end{aligned} \tag{4.2}$$

where capital indices indicate absolute magnitudes from Forbes & Short (1996), and lowercase indices denote differential magnitudes from this study. The transformation coefficients are given by A and C, and the zero points by B and D. Figure 4.12 shows the graphs of 'V-v' as function of 'b-v' and 'B-V' as function of 'b-v', from which the transformation coefficients and zero points were determined by fitting the data with the above presented calibration equations. The transformation coefficients and zero points are given by $A = -0.156 \pm 0.018$, $B = 9.190 \pm 0.007$, $C = 1.058 \pm 0.014$ and $D = 0.580 \pm 0.005$

After the calibration was done, a colour magnitude diagram was constructed by using stars from the master list that was created in this study. The colour magnitude diagram was then used as basis for identifying individual stars from Forbes & Short (1996), who identified a total number of 104 stars from both NGC 6204 and Hogg 22. Figure 4.13 shows these stars from Forbes & Short (1996) on the colour magnitude diagram overplotted on the stars from this study which are shown in red. The two clusters can clearly be distinguished at the top of the main sequence where the NGC 6204 and Hogg 22 stars from Forbes & Short (1996) are represented by blue and green crosses respectively. The blue squares to the right of both clusters' main sequence indicate stars which, according to Forbes & Short (1996), belong to NGC 6204, but by inspection of their position on the diagram, their cluster membership is strongly questioned and as a result they are identified as possible field stars. These field stars were then identified newline

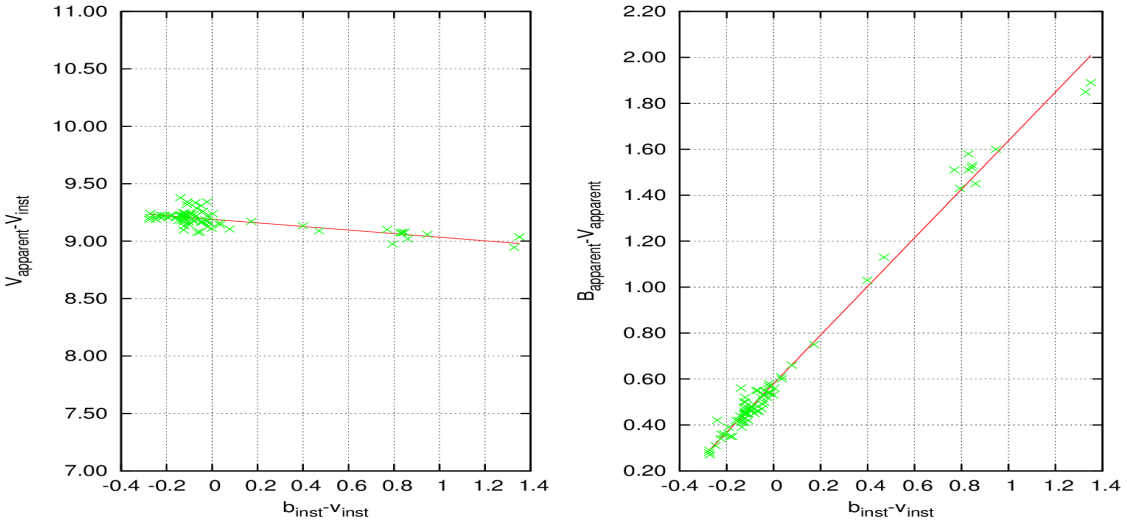

FIGURE 4.12: The relation between the (B-V) and (V-v) colors to (b-v), showing the color transformation by using B and V magnitudes obtained from Forbes & Short (1996).

from the data set of the current study and indicated on a diagram from Forbes & Short (1996), shown in Figure 4.14.

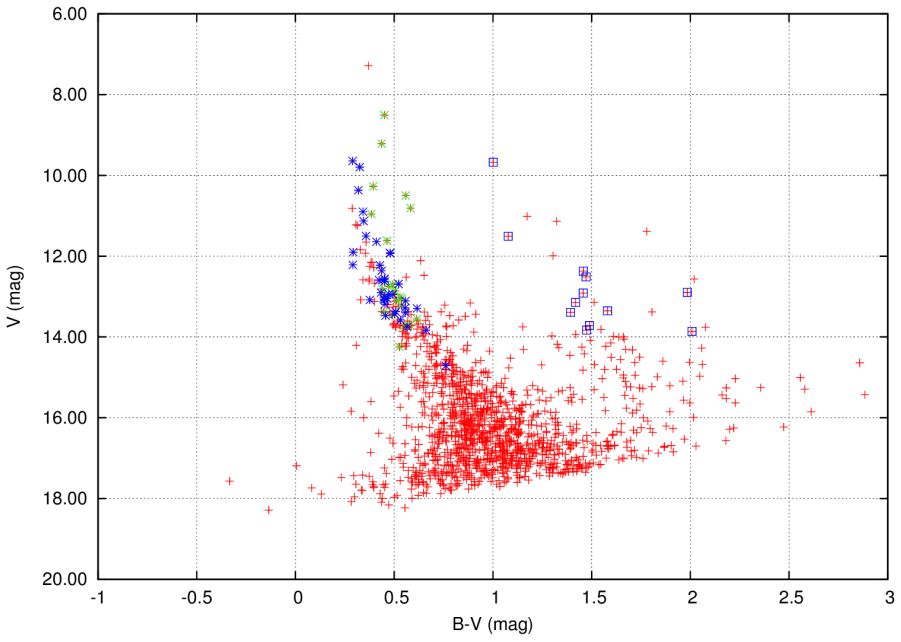

FIGURE 4.13: Color magnitude diagram of all stars from the photometry master list (red) together with identified cluster members from Forbes & Short (1996) (NGC 6204: blue; Hogg 22: green).

Isochrones for 3.66×10^7 years and 6.03×10^6 years, using the online Padova database of stellar evolutionary tracks and isochrones based on tracks from Marigo et al. (2008), were plotted for NGC 6204 and Hogg 22 respectively, where the ages for both clusters were obtained from the WEBDA galactic open cluster database. The isochrones were

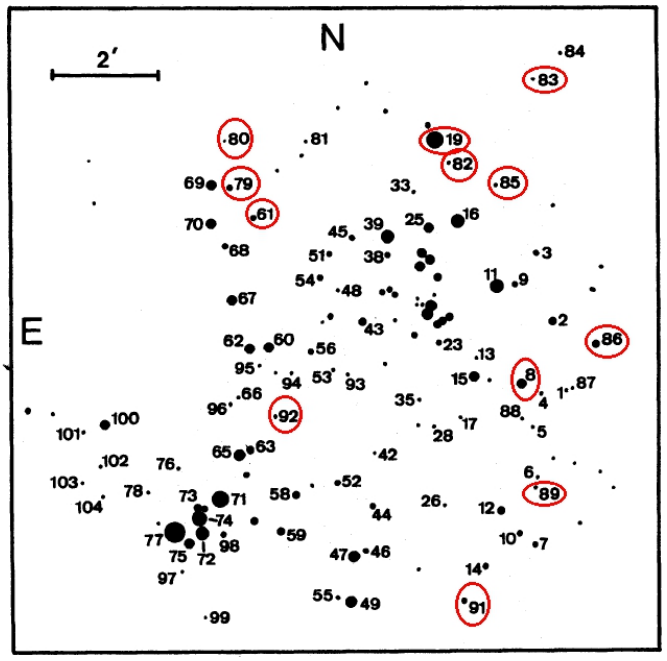

FIGURE 4.14: Possible field stars identified on the cluster diagram from Forbes & Short (1996)

corrected for extinction and distance, where the V-band extinction A_v for Hogg 22 and NGC 6204 was calculated, using information from the WEBDA database, to be 2.0 and 1.33 respectively (see Appendix A for calculation). The isochrones were plotted on the colour magnitude diagram which is shown in Figure 4.15 together with stars from both clusters and the field stars mentioned above. The calibration process made it possible to identify stars of particular interest to this study, which were observed by Forbes & Short (1996).

The two stars that were mentioned earlier in this section, which are possible candidate β Cephei stars, are indicated on the two colour diagram (Figure 4.16) from Forbes & Short (1996), together with the known β Cephei star, id11. From the reddening vector on the figure, it is clear that the three indicated stars have approximately the same spectral type, which is a good indicator that id13 and id22 belong to the class of β Cephei stars (private communication).

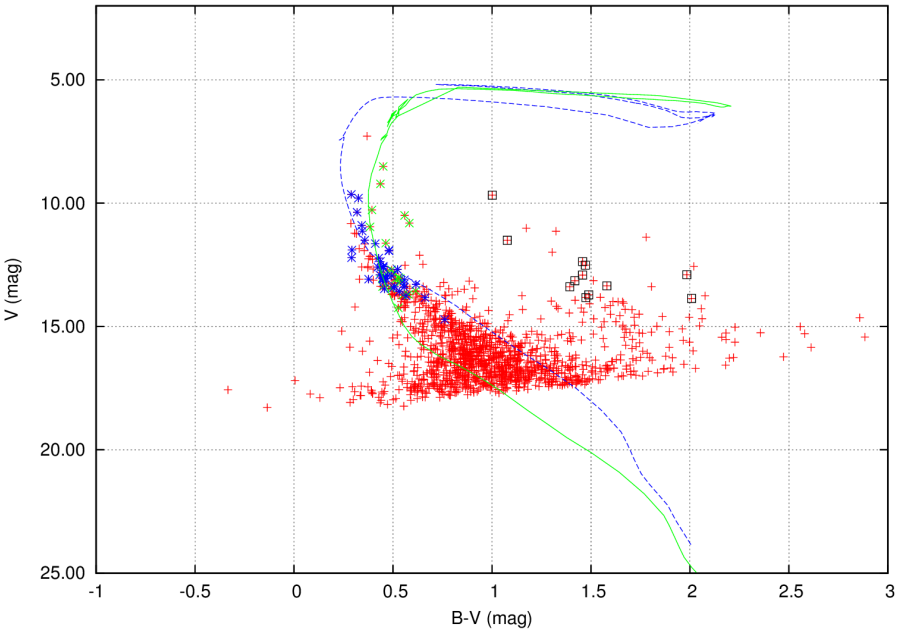

FIGURE 4.15: Colour magnitude diagram showing cluster members from Forbes & Short (1996), all stars from this study (red), and isochrones overplotted to each cluster as described in the text (NGC 6204: blue; Hogg 22: green).

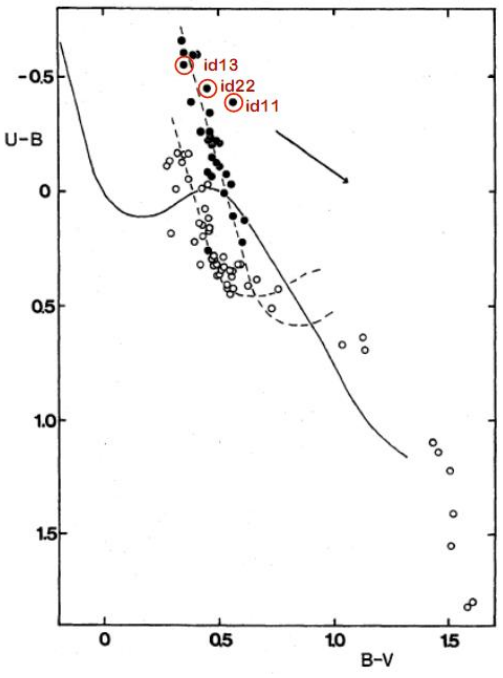

FIGURE 4.16: Two possible β Cephei stars together with one known β Cephei star in Hogg 22, indicated on the two colour diagram from Forbes & Short (1996). The reddening arrow is indicated on the diagram, showing that these three stars have the same spectral type.